Chinese Chemical Letters 37 (2026) 112015

Contents lists available at ScienceDirect

Chinese Chemical Letters

journal homepage: www.elsevier.com/locate/cclet

Synthesis of hyperbranched polymers from epoxide and acrylate: An effective polyether/polyacrylate compatibilizer

Wei Wang[a], Tian-Jun Yue[a,*], Xiang-Yu Fu[a], Xiao-Hui Guo[a], Ge-Ge Gu[b], Xiao-Bing Lu[a], Wei-Min Ren[a]

[a] State Key Laboratory of Fine Chemicals, Frontiers Science Center for Smart Materials, Dalian University of Technology, Dalian 116024, China
[b] Instrumental Analysis Center, Dalian University of Technology, Dalian 116024, China

ARTICLE INFO

Article history:
Received 26 August 2025
Revised 18 October 2025
Accepted 20 October 2025
Available online 23 October 2025

Keywords:
Epoxides
Acrylates
Hyperbranched polymers
Compatibilizer
Bimetallic synergistic catalysis
Isotactic polyether

ABSTRACT

Hyperbranched polymers (HBPs) comprising polyether and polyacrylate segments are effective for enhancing the performance of polyether and polyacrylate blends. However, this approach is limited by difficulties associated with efficient synthetic strategies and structural modifications. Herein, we develop a strategy for synthesizing HBPs through the copolymerization of epoxides and acrylates, wherein glycidyl acrylate (GA), a bifunctional monomer comprising epoxy and acrylate groups, was added as the branching point. The dinuclear Cr-complex-catalyzed copolymerization of epoxides and acrylates occurred in a monomer reactivity-determined manner. By varying the feed ratio of GA, HBPs with various branching degrees were accessed, attaining HBPs with different molecular weights. Furthermore, the obtained HBPs are effective in promoting the mechanical performances of polyether and polyacrylate blends. Morphological characterization revealed that the incorporation of HBPs into blends improved the microphase fusion of immiscible domains within the blend, highlighting their excellent compatibilization performances.

© 2026 Published by Elsevier B.V. on behalf of Chinese Chemical Society and Institute of Materia Medica, Chinese Academy of Medical Sciences.

The versatile architectures of polymeric materials impart them with highly programming properties, thus enabling their various applications [1–3]. The architectures of polymers include linear, cyclic, hyperbranched, star-shape, and cross-linked structures [4,5], which originate from different connection ways of various polymer segments. Among these architectures, branched polymers, owing to their irregular three-dimensional topology, exhibit unique properties compared to their linear counterparts. These include rheological differences such as reduced chain entanglement, as well as higher solubility, weaker mechanical strength, and distinct self-assembly behaviors [6,7]. Particularly, branched polymers, owing to their ability to stitch domains together by repeatedly crossing the interface between two homopolymers, are effective compatibilizers for promoting the interfacial adhesion between two immiscible polymers, thus enhancing their mechanical performances [8–10]. Therefore, it is important to develop an effective strategy for synthesizing polymers with branched structures to extend the library of branched polymer compatibilizers.

Traditionally, the well-established strategy for synthesizing branched polymers mainly includes grafting strategies, that is, "grafting to", "grafting through", and "grafting from" [11]. However, these strategies often necessitate the pre-synthesis of side- or main-chains, leading to tedious synthetic procedures [12]. Much effort has been devoted to develop facile and efficient synthetic methods to attain branched polymers [13–15]. Two elegant strategies have been established through the: (i) *In situ* construction of a reactive group end-capped oligomer as a side chain for synthesizing branched polymers [16,17], and (ii) utilization of bifunctional monomers, *i.e.*, monomers containing two reactive groups, as branching point for synthesizing hyperbranched polymers (HBPs) [18–20]. An example of the former is that branched poly(monothiocarbonate) can be accessed from epichlorohydrin and carbonyl sulfide (COS) *via* the *in situ* synthesis of poly(monothiocarbonate) oligomer end-capped with an epoxy group, which acts as branching point. The terpolymerization of COS with epichlorohydrin and epoxy at elevated temperature generates branched sulfur-containing polymers [21]. The use of bifunctional monomers for synthesizing HBPs represents a more general method [22–25]. For example, 1,3,4-benzene tricarboxylic anhydride was used as a branching point to produce hyperbranched

* Corresponding author.
E-mail address: tjyue189@dlut.edu.cn (T.-J. Yue).

https://doi.org/10.1016/j.cclet.2025.112015
1001-8417/© 2026 Published by Elsevier B.V. on behalf of Chinese Chemical Society and Institute of Materia Medica, Chinese Academy of Medical Sciences.

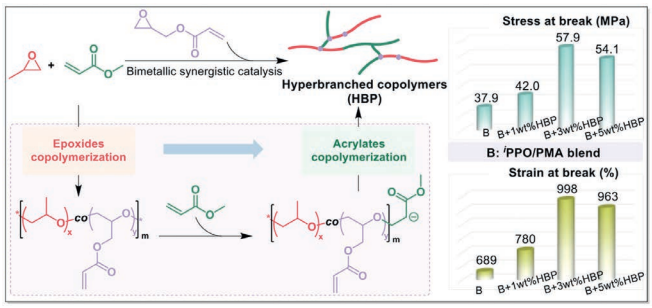


Fig. 1. Proposed strategy for the synthesis of hyperbranched ^{i}PPO-*b*-PMA block copolymer for compatibilizer applications.

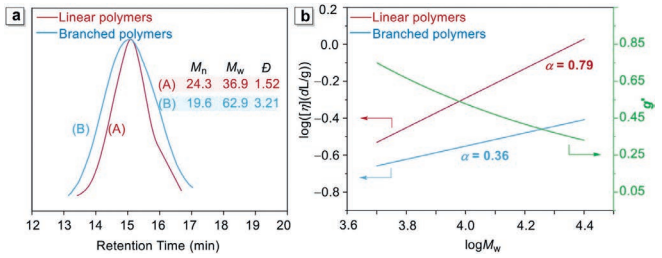


Fig. 2. Comparison between BCP (linear) and HBP1 (branched): (a) GPC traces; (b) Mark–Houwink plots, contraction factor: $g' = [\eta]_{br}/[\eta]_{lin}$ (green line). M_n and M_w are given in kg/mol.

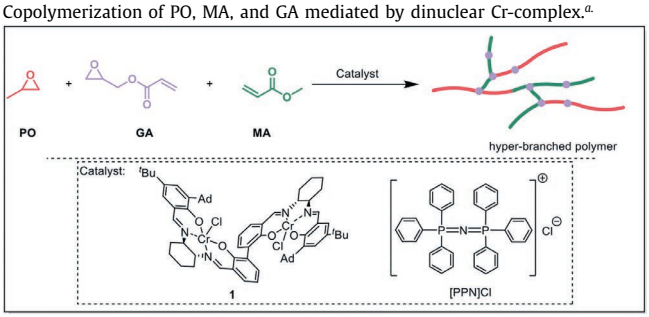
polyether-*b*-polycarbonate copolymers [25]. These well-established synthetic methodologies enable the development of functional HBPs from low-cost, readily available monomers, thereby facilitating the high-value utilization of fundamental compounds.

Epoxides and acrylates are two fundamental chemicals that have been widely used in many areas [26,27], with one of the important applications being to produce polymers [28,29]. In particular, the direct construction of polymeric materials from epoxides and acrylates represents an elegant strategy for attaining functional polymers [30–32]. For example, Wang *et al.* described an effective strategy for synthesizing block copolymers comprising polyacrylates and epoxide-derived copolymers using switchable polymerization [33,34]. Very recently, we achieved the sequence-controlled copolymerization of epoxides and acrylates using a bimetallic synergistic catalysis strategy [35], by which multiblock copolymers comprising polyester and polyacrylate segments can be synthesized for use as compatibilizers [36]. In addition, hyperbranched poly(glycidyl acrylate), which can be used for enhancing the performance of epoxy thermosets, can be synthesized *via* a photomediated switchable polymerization from epoxide, acrylate, and epoxy-capped acrylate [37]. Nevertheless, the direct synthesis of HBPs comprising polyether and polyacrylate has not yet been achieved. Our previous work indicated that bimetallic synergistic catalysis was capable of facilitating the copolymerization of epoxides and acrylates for synthesizing block copolymers, wherein the homopolymerization of epoxide proceeded first, followed by the homopolymerization of acrylate with the initiation of an alkoxide [35]. We envision that the introduciton of glycidyl acrylate (GA), a bifunctional monomer comprising both epoxy and acrylate groups, into the copolymerization of epoxides and acrylates is viable for synthesizing HBPs. In this procedure, the copolymerization of propylene oxide (PO) and GA proceeded first, forming a polyether with attached acrylate groups (Fig. 1). Then, the copolymerization of the acrylate groups occurred after the epoxide groups were fully consumed with the initiation of alkoxide, generated from the ring-opening polymerization (ROP) of epoxide. Herein, we aimed to synthesize HBPs comprising polyether and polyacrylate through the copolymerization of PO and methyl acrylate (MA) in the presence of GA using a bimetallic catalysis strategy. Varying the GA addition amount enables the production of HBPs with different branching degrees, which can be used as effective compatibilizers for enhancing the mechanical performances of polyether/polyacrylate blends.

Dinuclear SalenCrCl complex (**1**) in conjunction with [PPN]Cl (PPN = bis(triphenylphosphine)iminium) was employed to catalyze the copolymerization of PO, GA, and MA with a feed ratio of PO:MA:GA:**1**:[PPN]Cl = 1000:1000:3:1:2 at 60 °C. The polymerization proceeded efficiently, as all the monomers were almost fully consumed within 5 h (Table 1, entry 1). Hydrogen nuclear magnetic resonance (^{1}H NMR) spectroscopy characterization revealed that the resulting copolymer comprised poly(propylene oxide) (PPO) and poly(methyl acrylate) (PMA) segments (Fig. S1 in Supporting information). In addition, the number-average molecular weight (M_n) of the resulting polymer (HBP1) was 19.6 kg/mol with a dispersity ($Đ$) of 3.21. In contrast, the copolymerization of PO and MA catalyzed by **1**/[PPN]Cl yielded the corresponding PPO-*b*-PMA block copolymer (BCP) with an M_n of 24.3 kg/mol and a narrowed $Đ$ of 1.56 (entry 2). However, the weight-average molecular weight (M_w) of HBP1 was higher than that of BCP (62.9 *vs.* 37.9 kg/mol), indicating the formation of branched structure of resulting copolymers (Fig. 2a). To verify this hypothesis, detailed comparisons regarding the relationship between M_w and intrinsic viscosity of HBP1 and BCP was conducted using gel permeation chromatography (GPC) equipped with triple detectors, including refractive index, intrinsic viscosity, and two light scattering detectors. According to Mari–Houwink plots recorded by GPC, the Mark–Houwink exponents (α) of HBP1 and BCP were 0.36 and 0.79 (Fig. 2b), respectively, characteristic of a randomly branched and linear polymer. The branched characteristics of HBP1 is further evidenced by the fact that the contraction factor (g′), *i.e.*, the ratio of the intrinsic viscosities of HBP1 and BCP, decreased with increasing M_w. Taken together, these results confirmed that HBP1 possesses a hyperbranched structure.

Subsequently, we focused on synthesizing HBPs with different branching degrees by varying the feed ratios of GA. Increasing the GA:**1** feed ratio from 3:1 to 6:1, 9:1, and 12:1 resulted in no obvious change in the M_ns (from ~23.1 kg/mol to 24.8 kg/mol) of the resulting copolymers; whereas, $Đ$s increased from 3.21 to 7.66, 8.10, and 12.10, respectively (entries 3–5, Table 1). Correspondingly, M_ws of the resulting copolymers increased to 189.9, 197.6, and 279.5 kg/mol, respectively, indicating the branched density of the resulting copolymers increased with the GA addition amount. Nevertheless, further improving the GA:**1** feed ratio to 15:1 led to the gelation of the resulting copolymers (entry 6). In addition, at the lower catalyst concentration with a feed ratio of PO:MA:GA:**1**:[PPN]Cl = 4000:4000:24:1:2, the copolymerization decelerated, as it required 12 h to attain PO and MA conversions of 99% and 98%, respectively. Compared with the copolymerization with a feed ratio of PO:GA = 1000:6 (HBP2, entry 3), M_n of the resulting copolymer increased to 34.6 kg/mol, but with a lower $Đ$ of 4.37, indicating a lower M_w (151.2 *vs.* 189.9 kg/mol) of the resulting copolymer (entry 7, Table 1). This might be attributed to the relatively lower reactivity of GA under a lower catalyst concentration. This hypothesis was further evidenced by the fact that $Đ$ of the copolymer synthesized with a higher GA feed ratio of 4000:4000:30:1:2 was lower than that of HBP2 (7.66 *vs.* 7.15) (entry 8, Table 1). The decelerated copolymerization led to a decreased PO conversion of 72%, producing branched copolymer with a higher M_w of 320.3 kg/mol. Similarly, the gelation was observed as GA addition was increased to 4000:4000:40:1:2 (entry 9, Table 1). In addition, the copolymerization was also capable of proceeding under lower catalyst loading, affording a lower PO conversion and branched copolymer with decreased M_w (entry 10, Table 1).

Table 1
Copolymerization of PO, MA, and GA mediated by dinuclear Cr-complex.[a]



Entry	PO/MA/GA/**1**/PPNCl	Time (h)	Conv. [b] (%)			M_n [c] (kg/mol)	M_w [d] (kg/mol)	$Đ$ [c] (M_w/M_n)
			PO	MA	GA			
1	1000/1000/3/1/2	5	99	99	>99	19.6	62.9	3.21
2	1000/1000/0/1/2	5	99	98	–	24.3	37.9	1.56
3	1000/1000/6/1/2	4	99	99	>99	24.8	189.9	7.66
4	1000/1000/9/1/2	5	99	99	>99	24.4	197.6	8.10
5	1000/1000/12/1/2	3	99	99	>99	23.1	279.5	12.10
6 [d]	1000/1000/15/1/2	3	–	–	–	n.d. [e]	n.d.	n.d.
7	4000/4000/24/1/2	12	99	99	98	34.6	151.2	4.37
8	4000/4000/30/1/2	12	72	90	99	44.8	320.3	7.15
9 [d]	4000/4000/40/1/2	12	–	–	–	n.d.	n.d.	n.d.
10	6000/6000/30/1/2	12	31	77	99	24.6	167.3	6.80

[a] Conditions: Reactions were performed in PO (10 mmol) and MA (10 mmol) with the addition of GA (feed ratio as noted) in a 25-mL flask at 60 °C. Toluene was added as the solvent at a mass ratio of $m_{(toluene)}$:$m_{(PO+GA)}$ = 2:1.
[b] The conversion of monomers and structure of the copolymer were determined using ^{1}H NMR spectroscopy.
[c] Determined by GPC in tetrahydrofuran and calibrated with polystyrene.
[d] The reaction mixture presented as an insoluble solid due to the gelation of the resulting copolymer in the presence of high GA content.
[e] n.d. = Not detected.

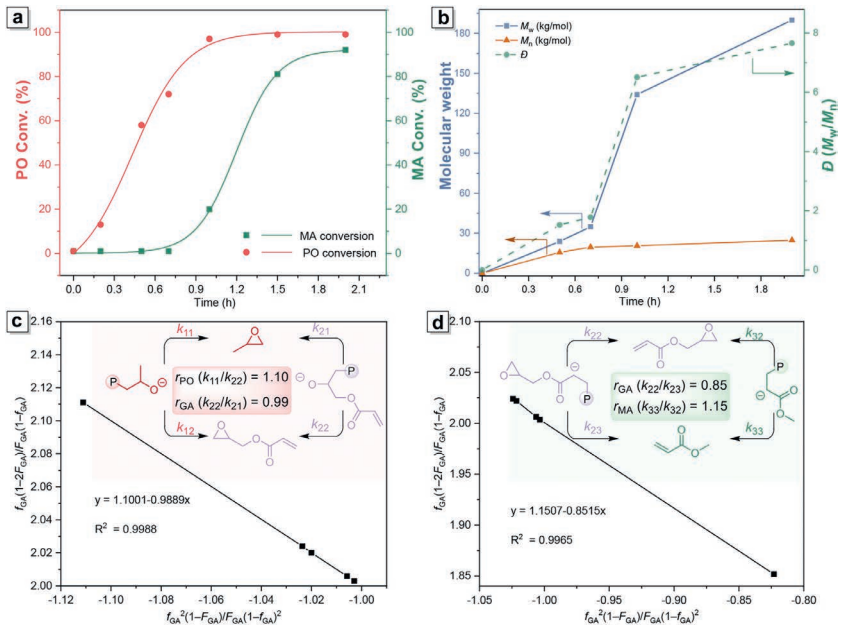


Fig. 3. Copolymerization process study: Variation in (a) PO and MA conversion and (b) molecular weights and dispersities with time; Fineman–Ross plot and kinetic parameters for the copolymerization of (c) PO and GA and (d) GA and MA mediated by the **1**/PPNCl catalyst system.

This can be attributed to the lower transformation efficiency of PO at a lower catalyst concentration.

To shed more light on how the HBPs were produced, the copolymerization process of PO and MA in the presence of GA was monitored *via* an intermittent experiment. A series of parallel experiments with a feed ratio of PO:MA:GA:**1**:[PPN]Cl = 500:500:3:1:2 were performed and quenched at different times, and the reaction mixtures were extracted for ^{1}H NMR and GPC analyses. Only PO conversion was observed during the initial stage (Fig. 3a). Notably, no signal representing GA was observed (Fig. S2 in Supporting information), which can be attributed to its concentration being too low to be detected during the polymerization process. M_ns of the resulting polymers increased as PO was consumed and reached 19.6 kg/mol with a $Đ$ of 1.78 (Fig. 3b). Then, the transformation of MA occurred after PO was fully consumed. Correspondingly, M_n of resulting copolymer dramatically increased as MA was consumed, together with an increase in $Đ$, indicating the formation of a branched copolymer.

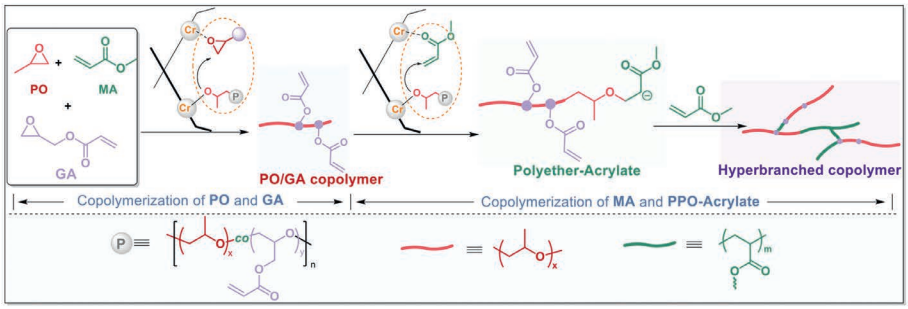


Fig. 4. Proposed mechanism for the synthesis of HBPs *via* the dinuclear Cr-complex-catalyzed copolymerization epoxides and acrylate in the presence of GA.

To obtain more structural information on the branched points of the resulting copolymer, the competition rates of the monomer sets PO/GA and GA/MA were explored. The monomer reactivity ratios of PO/GA and GA/MA copolymerizations were established according to the Fineman–Ross equation (Tables S1 and S2 in Supporting information). r_{PO} and r_{GA} were determined to be 1.10 and 0.99, respectively, from the copolymerization of PO and GA (Fig. 3c). The higher reactivity of PO compared with that of GA indicates that the PO insertion is more favored, indicating that GA is distributed at the end of polymer mainchain. Similarly, r_{GA} and r_{MA} were determined to be 0.85 and 1.15, respectively, from the copolymerization of GA and MA (Fig. 3d), indicating that the insertion of MA was more favored. Consequently, the addition of small amounts of GA (up to 0.12%, in molar ratio) led to the formation of HBPs comprising polyether and polyacrylate segments.

Accordingly, the HBPs synthesis mechanism is proposed to be as follows. In the copolymerization process, due to the low addition amount of GA, the random copolymerization of PO and GA occurred first, forming polyether segments with acrylate groups distributed at the end of polyether segments (Fig. 4). Then, the propagating species of alkoxylate triggered the copolymerization of MA and acrylate groups appended to the polyether segment. Therefore, HBPs comprising polyether and polyacrylate segments were produced from the copolymerization of PO and MA in the presence of GA, in which GA acted as the branching point.

In addition, substituting (*rac*)-PO for optical (*S*)-PO to copolymerize with MA in the presence of GA (^{i}PO:GA = 1000:6) produced a HBP (^{i}HBP1) with an isotactic PPO (^{i}PPO) segment (Table S3 in Supporting information), of which the isotacticity reached 85% (Fig. S3 in Supporting information). Differential scanning calorimetry (DSC) characterization revealed that ^{i}HBP1 has a melting temperature (T_m) of 67.5 °C, ascribed to the ^{i}PPO segment, together with two glass transition temperatures (T_gs) of −73.4 and 8.6 °C (Fig. S4 in Supporting information) [36,38]. With this HBP in hand, we attempted to extend its application in facilitating the compatibilization of immiscible ^{i}PPO/PMA blends, in which ^{i}PPO and PMA were synthesized from the respective homopolymerization of (*S*)-PO and MA, respectively, thereby improving their mechanical properties (Fig. 5a). Initially, the thermal and mechanical performances of ^{i}PPO/PMA blends with different ratios were characterized using DSC and universal tensile tests. The ^{i}PPO/PMA blend (70:30 wt%, **B1**) has a T_m and T_g of 67.6 and 18.4 °C, respectively (Fig. 5b), ascribed to ^{i}PPO and PMA. This is in good accordance with the T_m and T_g of isolated PPO and PMA, respectively (Fig. S5 in Supporting information). No difference in T_m and T_g between the blend and isolated ^{i}PPO and PMA indicates that **B1** has a separated microphase.

Tensile text revealed that **B1** has an ultimate tensile strength (σ_b) and strain (ε_b) at break of 37.9 MPa and 689%, respectively (Fig. 5c). Subsequently, ^{i}HBP1 with a weight content of 3 wt% was added to **B1** to improve its mechanical performance (**B2**). The addition of ^{i}HBP1 had no obvious influence on the thermal properties of **B2**, which exhibited a T_m of 64.9 °C and T_gs of −66.7 and 18.1 °C. However, σ_b and ε_b of **B2** were improved to 53.2 MPa and 889%, respectively. After the addition of 3 wt% ^{i}PPO-*b*-PMA block copolymer (^{i}BCP to **B1**), σ_B and ε_b of **B3** were lower than those of **B2** (53.2 *vs.* 43.4 MPa and 889% *vs.* 761%, respectively). This suggests that the topological structure of the ^{i}PPO-*b*-PMA block copolymer significantly influenced its compatibilization efficiency in enhancing the mechanical performance of the ^{i}PPO/PMA blend, with higher branching degrees yielding greater efficiency. To verify this hypothesis, we examined the thermal and mechanical properties of PO/MA blends containing block copolymers with different branching degrees that were synthesized through PO/MA copolymerization in the presence of GA at (*S*)-PO:GA feed ratios of 1000:12 (^{i}HBP2) and 4000:30 (^{i}HBP3). DCS characterization revealed no obvious change in T_m and T_g of the blends (Fig. 5b). Blends comprising block copolymers with higher branching degrees exhibited enhanced mechanical properties, as σ_bs improved from 37.8 (**B1**) to 53.5 (**B4**) and 57.9 MPa (**B5**), with a corresponding increase in ε_bs from 689% to 981% and 998%, respectively (Fig. 5c). These results revealed that block copolymers with higher branching degrees exhibit higher compatibilization efficiency, with ^{i}HBP3 demonstrated to be the most effective compatibilizer.

Subsequently, the influence of the ^{i}HBP3 content on the compatibilization efficiency were explored in detail. ^{i}HBP3 incorporation had no significant effect on the thermal properties of the resulting blends. Two glass transitions (from −65.0 °C to −64.0 °C and from 16.7 °C to 18.4 °C) and a melting peak near 66.0 °C were observed from the second-heating DSC curves for blends containing different amounts of ^{i}HBP3 (Fig. 6a). Characterizing the blends using dynamic mechanical analyzer (DMA) revealed comparable loss factors (tan δ) for all blends. However, the storage modulus (E') of the blends increased with a higher ^{i}HBP3 content (Fig. 6b). Notably, **B5** (**B1** containing 3 wt% ^{i}HBP3) achieved the highest E' of 4350 MPa at −75.0 °C. Reducing the amount of ^{i}HBP3 to 1 wt% (**B6**) reduced the compatibilization efficiency, yielding a σ_b and ε_b of 42.0 MPa and 780%, respectively (Fig. 6c). While incorporating 5 wt% ^{i}HBP3 into **B1** (**B7**) enhanced its mechanical properties (σ_b = 54.1 MPa, ε_b = 963%), these values remained lower than those of **B5**. Collectively, these results indicate that 3 wt% ^{i}HBP3 optimally improved the mechanical performance of the ^{i}PPO/PMA blend. To elucidate how ^{i}HBP3 enhances the mechanical performances of the ^{i}PPO/PMA blend, the morphologies of blends containing varying ^{i}HBP3 contents were characterized using scanning electron microscopy (SEM) and atomic force microscopy (AFM). SEM characterization revealed the sea-island structure of the ^{i}PPO/PMA blend, indicating that immiscible domains were formed due to the separated microphase of ^{i}PPO/PMA (Fig. 6d, **B1**). In contrast, incorporating hyperbranched ^{i}PPO-*b*-PMA block copolymer improved microphase separation, which was evidenced by the smoother, flatter morphologies observed for the ^{i}PPO/PMA blends containing ^{i}HBP3. Specifically, the blend with 3 wt% ^{i}HBP3 (**B5**) exhibited the most uniform microphase, which

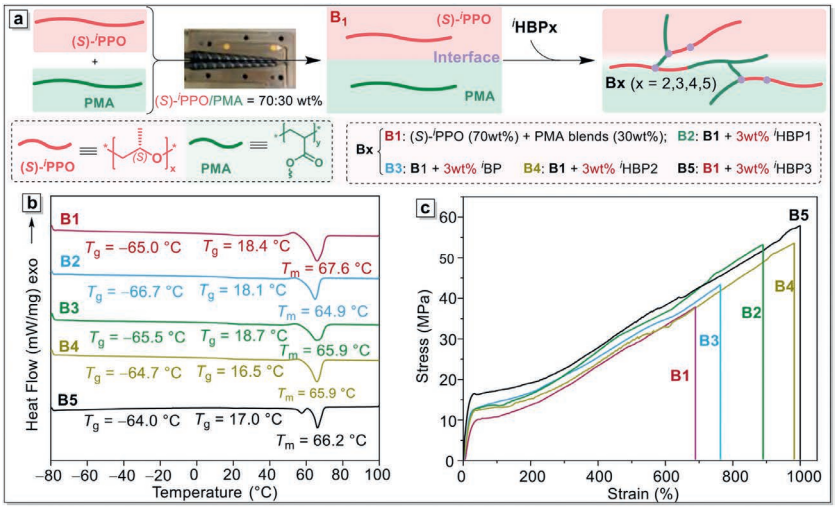


Fig. 5. Preparation and properties characterization of different ^{i}PPO /PMA blends: (a) Schematic diagram of preparation of blends containing different HBPs; (b) DSC curves and (c) stress–strain plots of PPO/PMA blends incorporated with different hyperbranched PO/MA copolymers: **B1**: ^{i}PPO/PMA = 70:30 (wt%); **B2**: **B1** + 3 wt% ^{i}HBP1; **B3**: **B1** + 3 wt% ^{i}BCP; **B4**: **B1** + 3 wt% ^{i}HBP2; **B5**: **B1** + 3 wt% ^{i}HBP3.

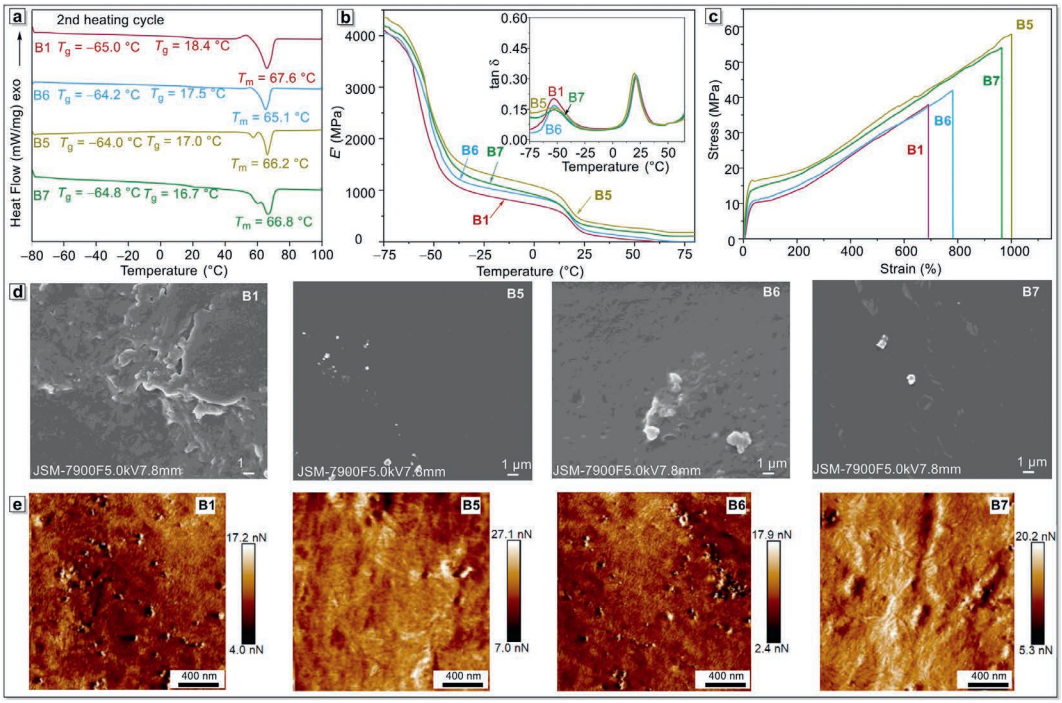


Fig. 6. Properties of PCP/PMA blends with different amounts of HBPs: (a) DSC curves; (b) storage moduli and tanδ; (c) stress–strain curves; (d) SEM images; and (e) AFM images. **B1**: ^{i}PPO/PMA = 70:30 (wt%); **B5**: **B1** + 3 wt% ^{i}HBP3; **B6**: **B1** + 1 wt% ^{i}HBP3; **B7**: **B1** + 5 wt% ^{i}HBP3.

was further supported by AFM imaging (Fig. 6e), highlighting its superior ability to promote microphase fusion. These findings indicate that ^{i}HBP3 addition reduces interfacial tension and domain size within the ^{i}PPO/PMA blend, thereby enhancing its mechanical performance.

In summary, we have demonstrated an effective strategy for synthesizing HBPs from epoxides and acrylate *via* bimetallic synergistic catalysis in the presence of GA. This strategy is supported by the monomer reactivity-determined polymerization in the presence of GA, with the random copolymerization of epoxide and GA occurring first. Notably, the branching degree of the resulting HBP can be readily tuned by changing the amount of GA. In addition, the incorporation of HBPs improved the mechanical performances of the blend comprising ^{i}PPO and PMA. A detailed investigation of the influence of the topological structure and weight content of HBPs revealed the structure–performance relationship, indicating their excellent potential for use as compatibilizers.

CRediT authorship contribution statement

Wei Wang: Writing – original draft, Methodology, Investigation, Formal analysis, Data curation. **Tian-Jun Yue:** Writing – review & editing, Supervision, Funding acquisition, Formal analysis. **Xiang-Yu Fu:** Methodology, Formal analysis, Data curation. **Xiao-Hui Guo:** Formal analysis, Data curation. **Ge-Ge Gu:** Software, Data curation. **Xiao-Bing Lu:** Writing – review & editing, Funding

acquisition. **Wei-Min Ren:** Writing – review & editing, Supervision, Funding acquisition, Conceptualization.

Declaration of competing interest

The authors declare that they have no known competing interests or personal relationships that could have appeared to influence the work reported in this paper.

Acknowledgments

This work was supported by National Natural Science Foundation of China (No. 22171037 to W.-M. Ren), the Fundamental Research Funds for the Central Universities (Nos. DUT25RC(3)021, DUT25Z2724, and DUT22LAB609 to T.-J. Yue) and the National Key Research and Development Program of China (No. 2021YFA1501704).

Supplementary materials

Supplementary material associated with this article can be found, in the online version, at doi:10.1016/j.cclet.2025.112015.

References

[1] Y. Gao, D. Zhou, J. Lyu, et al., Nat. Rev. Chem. 4 (2020) 194–212.
[2] G. Polymeropoulos, G. Zapsas, K. Ntetsikas, et al., Macromolecules 50 (2017) 1253–1290.
[3] Y. Gu, E.A. Alt, H. Wang, X. Li, A.P. Willard, J.A. Johnson, Nature 560 (2018) 65–69.
[4] T.J. Yue, L.Y. Wang, W.M. Ren, Polym. Chem. 12 (2021) 6650–6666.
[5] K. Matyjaszewski, Adv. Mater. 30 (2018) 1706441.
[6] W. Wu, R. Tang, Q. Li, Z. Li, Chem. Soc. Rev. 44 (2015) 3997–4022.
[7] M.B. Sims, Polym. Int. 70 (2021) 14–23.
[8] C.R. López-Barrón, P. Brant, M. Shivokhin, et al., Macromolecules 51 (2018) 5720–5731.
[9] S.W. Zhou, C. Yu, M. Chen, et al., Smart Mol. 1 (2023) e20220009.
[10] Y. Chen, Y. Ding, P. Li, et al., Chin. J. Chem. 43 (2025) 1560–1567.
[11] R. d'Arcy, J. Burke, N. Tirelli, Adv. Drug Deliv. Rev 107 (2016) 60–81.
[12] F.L. Hatton, P. Chambon, T.O. McDonald, A. Owen, S.P. Rannard, Chem. Sci. 5 (2014) 1844–1853.
[13] X. Yan, X. Huang, Y. Liu, et al., Chin. Chem. Lett. 35 (2024) 109426.
[14] N. Ren, X. Wang, P. Sun, et al., Prog. Polym. Sci. 166 (2025) 101988–102023.
[15] Z. Li, H. Yong, K. Wang, et al., Chem. Commun. 59 (2023) 4142–4157.
[16] T.J. Yue, W.M. Ren, Y. Liu, Z.Q. Wan, X.B. Lu, Macromolecules 49 (2016) 2971–2976.
[17] B. Zhang, H. Li, H. Luo, J. Zhao, Eur. Polym. J. 134 (2020) 109820.
[18] H. Gao, K. Matyjaszewski, Prog. Polym. Sci. 34 (2009) 317.
[19] J. Zhang, G. Wang, Sci. China Chem. 58 (2015) 1674–1694.
[20] Y.Y. Cui, Y. Ren, X.X. Liu, Chin. Chem. Lett. 23 (2012) 985–988.
[21] T.J. Yue, G.A. Bhat, W.J. Zhang, et al., Angew. Chem. Int. Ed. 59 (2020) 13633–13637.
[22] O.B. Penrhyn-Lowe, S. Flynn, S.R. Cassin, et al., Polym. Chem. 12 (2021) 6472–6483.
[23] H. Zhao, C. Hu, X. Pang, X. Chen, Smart Mol. 2 (2024) e20240057.
[24] H. Gao, Chin. Chem. Lett. 30 (2019) 1996–2002.
[25] M. Zhao, S. Zhu, G. Zhang, et al., Macromolecules 56 (2023) 2379–2387.
[26] J. Herzberger, K. Niederer, H. Pohlit, et al., Chem. Rev. 116 (2016) 2170–2243.
[27] F. Bernard, G. Eyglunent, V. Daële, A. Mellouki, J. Phys. Chem. A 114 (2010) 8376–8383.
[28] M.I. Childers, J.M. Longo, N.J. Van Zee, A.M. LaPointe, G.W. Coates, Chem. Rev. 114 (2014) 8129–8152.
[29] B.K. Christopher, Macromol. Rapid Commun. 30 (2009) 1961–1963.
[30] Y. Wang, Y. Zhao, Y. Ye, et al., Angew. Chem. Int. Ed. 57 (2018) 3593–3597.
[31] K. Guo, S. Li, G. Chen, et al., CCS Chem. 4 (2022) 3134–3149.
[32] S. Zhu, Y. Zhao, M. Ni, et al., ACS Macro Lett. 9 (2020) 204–209.
[33] Y. Zhao, Y. Wang, X. Zhou, et al., Angew. Chem. Int. Ed. 58 (2019) 14311–14318.
[34] Y. Wang, Y. Zhao, S. Zhu, et al., Angew. Chem. Int. Ed. 59 (2020) 5988–5994.
[35] X.Y. Fu, T.J. Yue, B.H. Ren, et al., Angew. Chem. Int. Ed. 63 (2024) e202401926.
[36] X.Y. Fu, T.J. Yue, X.H. Guo, X.B. Lu, W.M. Ren, Nat. Commun. 16 (2025) 2154.
[37] S. Zhu, M. Zhao, H. Zhou, et al., Nat. Commun. 14 (2023) 1622.
[38] B.M. Lipinski, L.S. Morris, M.N. Silberstein, G.W. Coates, J. Am. Chem. Soc. 142 (2020) 6800–6806.